Chapter 4

Deconvolution

4.1 The convolutional model for seismic waves

Consider a simple earth model consisting of a stack of plane layers, (see Figure 4.1) where each layer has wave velocity c_k, density ρ_k and thickness d_k. k is here the number of a layer, with the top of layer $k = 0$ at $z = 0$, while the bottom of layer $k = N$ is at depth $z = z_N$. z is assumed positive downwards. Assume now that a seismic source is positioned at (or close to) the surface at $z = 0$. The source emits a source signal $s(t)$. The source signal will travel down to the bottom of layer no 0. Since layer no 1 generally have a different wave velocity and different density, part of the downgoing signal from the seismic source will be reflected and travel upward to the surface.

Assuming that the source signal only travels in the strict vertical direction (either straight up or straight down) the reflected signal is approximately described by

$$y(t) = r_0 \frac{s(t - \phi_0)}{2d}. \tag{4.1}$$

Here $\phi_0 = 2d_0/c_0$ is the two-way traveltime from the surface and down to the interface between layer no 0 and layer no 1. r_0 is the reflection coefficient given by

$$r_0 = \frac{c_1\rho_1 - c_0\rho_0}{c_1\rho_1 + c_0\rho_0}. \tag{4.2}$$

We see that the reflected signal according to equation 4.1 is just a scaled and time-delayed version of the signal $s(t)$ emitted by the source.

Part of the signal which impinges on interface 0 will be transmitted through the interface and down into layer no. 1. If we neglect the transmission loss, the signal will then travel to the bottom of layer no. 1 and part of this will be reflected and return along the same path to the surface. The signal recorded at

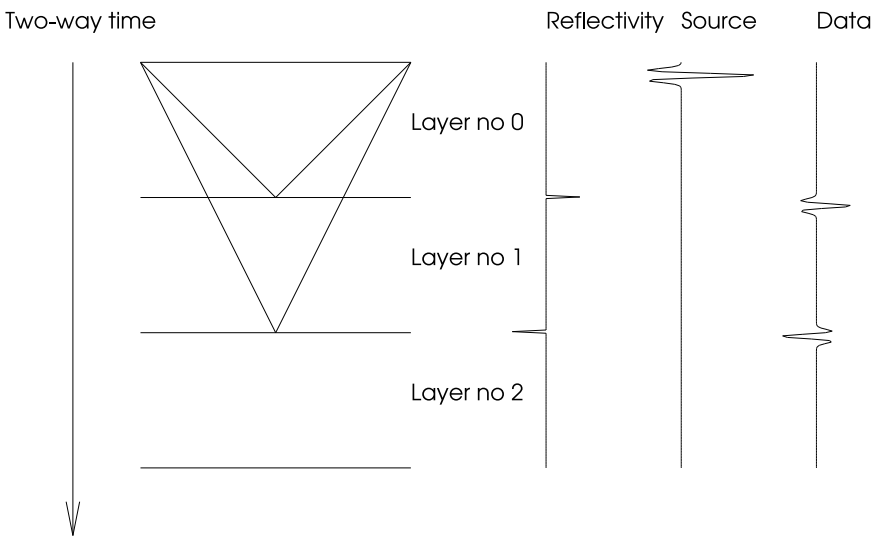

Figure 4.1: Layered earth model

the surface will then be

$$y(t) = r_0 \frac{s(t-\phi_0)}{2d_0} + r_1 \frac{s[t-(\phi_0+\phi_1)]}{2d_0+2d_1}, \tag{4.3}$$

where ϕ_1 is the two-way traveltime through layer no 1, while r_1 is the reflection coefficient for layer no 1. Equation 4.3 is very approximate since we have neglected all transmission losses and the geometrical spreading factor have been approximated with the distance, which is not strictly true, since geometrical spreading depends on the velocity in each layer. To make this model even simpler we will neglect the geometrical spreading by assuming that we are only considering reflections coming from interfaces far away from the source. The difference in geometrical spreading can then be neglected.

Based on equation 4.1 and equation 4.3 we can make a simple model for seismic waves reflected from all N layers by

$$y(t) = \sum_{k=0}^{N} r_k s(t-\tau_k), \tag{4.4}$$

where $\tau_k = \sum_{l=0}^{k} \phi_l$ is the two way traveltime from the surface and down to interface no k. If we now assume that the thickness and velocities of each layer is such that the two-way traveltime through each layer is the same and equal to Δt, then $\tau_k = k\Delta t$.

We see that equation 4.4 is really then a convolution since we can write

$$y_k = \sum_{l=0}^{N} r_l s_{k-l}, \tag{4.5}$$

where

$$\begin{aligned} y_k &= a(t = k\Delta t), \\ s_k &= s(t = k\Delta t). \end{aligned} \tag{4.6}$$

In the continuous case we can write

$$y(t) = \int_{\tau=0}^{+\infty} r(\tau)s(t-\tau), \tag{4.7}$$

if we assume $r(t < 0) = 0$. Equation 4.5 or 4.7 is the so-called convolutional model for seismic waves. It is an over-simplification of wave propagation, but for certain limited purposes it will prove to be very useful. Basically we assume that the earth can be described as a simple linear filter $r(t)$ and that wave propagation through the earth can be modelled as filtering the seismic source signal, $s(t)$, with the impulse response of the earth, $r(t)$.

4.2 Spiking deconvolution

Using the convolutional model for seismic waves we can describe a seismic trace $y(t)$ by

$$y(t) = r(t) * s(t), \tag{4.8}$$

where $s(t)$ is the seismic source and $r(t)$ is the reflection coefficient time series, which we will call the reflectivity.

Our primary aim is to recover $r(t)$ given that the seismic source $s(t)$ and the measured seismic trace $y(t)$ is known. Solving equation 4.8 is not straightforward, but if we Fourier transform equation 4.8 we get

$$Y(f) = R(f)S(f), \tag{4.9}$$

which can be trivially solved

$$R(f) = \frac{Y(f)}{S(f)}. \tag{4.10}$$

The Fourier transform of the reflectivity, $R(f)$, can actually be recovered by a spectral division.

Equation 4.10 can be slightly reformulated as

$$R(f) = S^{-1}(f)Y(f), \tag{4.11}$$

where $S^{-1} = 1/S(f)$ is an *inverse* filter.

When $S^{-1}(f)$ is applied to the input data it removes the effect of the source pulse and recovers the reflection coefficient.

Figure 4.2 shows the spectrum of a source pulse $|S(f)|$ and the inverse filter $|S(f)^{-1}|$.

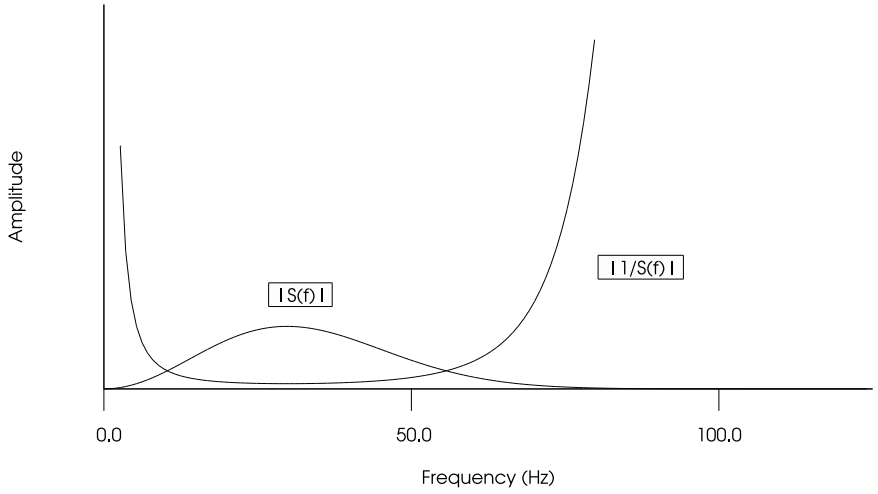

Figure 4.2: The spectrum of a Ricker pulse and it's inverse filter

Note that the inverse filter has very large amplitudes outside the frequency range of the source pulse.

If we apply the inverse filter in figure 4.2 to the synthetic data shown in Figure 4.1 using equation 4.11, after first Fourier transforming from time to frequency, we get the spectra shown in Figure 4.3. If we Fourier transform back to time we get the result shown in Figure 4.4.

The effect of the inverse filter is to transform the input data consisting of a sum of scaled and time delayed pulses into the reflectivity time series. We see that the spectrum of the output reflectivity series contains more frequencies than the input data, which has a limited frequency range. A real reflectivity series usually contains a much wider frequency range than seismic data, in fact an often used assumption is that the frequency spectrum of real reflectivity

series is *white*, i.e. the spectrum is more or less constant over the whole range of seismic frequencies.

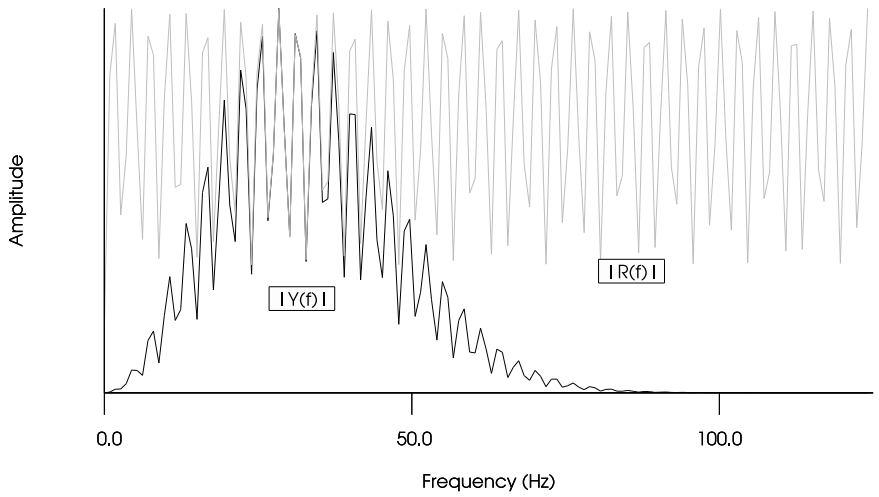

Figure 4.3: The spectrum of the input data $|Y(f)|$ and the deconvolved output $|R(f)|$ (gray line).

We are now in apparently good situation, a reasonably simple approach to recovering reflectivity from real data seem to work very well. However, in real seismic data there is usually noise (i.e. unwanted signal) in addition to the signal we are interested in. That implies that equation 4.9 should be replaced by

$$Y(f) = R(f)S(f) + N(f), \tag{4.12}$$

where $N(f)$ is a representation of the noise. An often used noise model is that of so-called white noise, which is a random signal with a constant amplitude spectrum.

Applying the inverse filter $S^{-1}(f)$ to the model in equation 4.12 gives

$$R(f) = S^{-1}(f)Y(f) - S^{-1}(f)N(f). \tag{4.13}$$

We see that there is now an extra term in the expression for the reflectivity involving the noise spectrum. The main problem here is that $S^{-1}(f)$ amplify the part of the noise spectrum which is outside the spectrum of the noise-free data. This is clearly seen in figure 4.5 which shows the spectrum of the input data and deconvolved data where white noise have been added to the input data. The corresponding input and output data in the time domain is shown in Figure 4.6. We see that the output deconvolution is completely unstable and

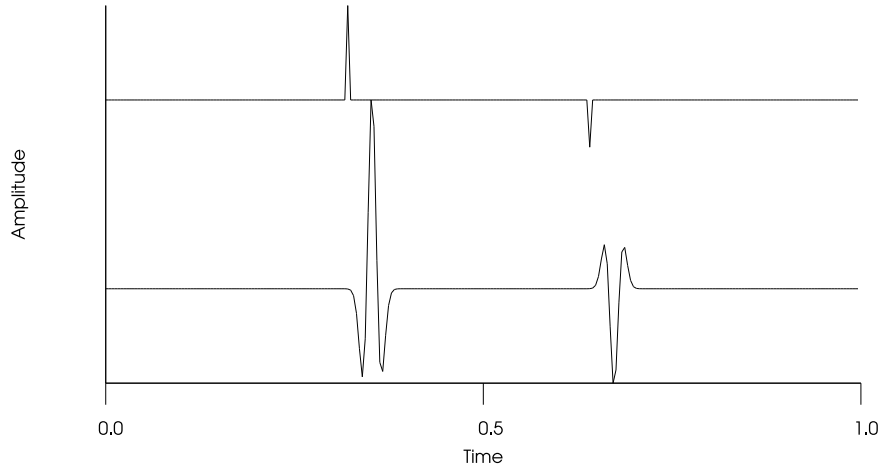

Figure 4.4: The input seismic data is shown in the lower trace, while the ouput of a spiking deconvolution filter applied to the input data is shown in the upper trace.

erroneous. It is clear that spectral division in the presence of noise in the input data does not really work. However, the situation can be rectified by observing that $S^{-1}(f)$ can be slightly modified by

$$S^{-1}(f) = \frac{1}{S(f) + \epsilon}, \tag{4.14}$$

where ϵ is a small constant designed to prevent $S^{-1}(f)$ becoming to large for frequencies outside the spectrum of $S(f)$. Figure 4.7 shows the spectrum of the same input data as in figure 4.6, but where $S^{-1}(f)$ have been stabilized by using equation 4.14 with $\epsilon = 0.1$. The corresponding result in the time domain is shown in figure 4.8. Comparing figures 4.6 and 4.8 wee see considerable improvement, and the result is no longer completely unstable.

4.3 Resolution and Bandwidth

The spiking deconvolution method described in the previous section can be thought of as a method to reshape the seismic pulse in the input data to a concentrated impulse (spike). This will increase the resolution, in the sense that the seismic reflectors in the deconvolved data is better separated than the seismic reflectors in the input data. Depending on the length of the seismic pulse, two reflectors may easily become indistinguishable if they are located close to each other. Figure 4.9 is an illustration of this effect. The lower trace is the reflectivity function used to create the synthetic seismic data shown in

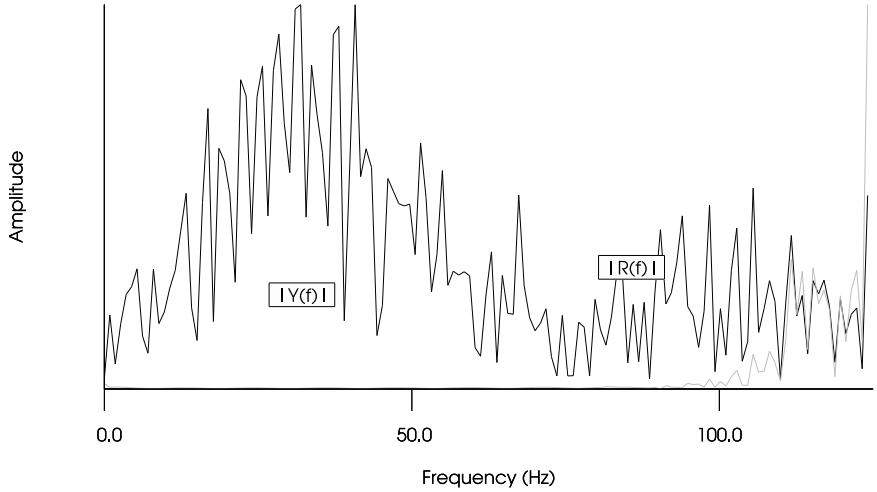

Figure 4.5: The spectrum of the input data with added noise $|Y(f)+N(f)|$ and the deconvolved output $|R(f)|$ (gray line).

the middle trace. We see that it is impossible to distinguish the two reflection coefficients in the data trace. However, if we apply a spiking deconvolution we recover the output as shown in the upper trace and the two reflectors again become possible to distinguish. Deconvolution act as a mean to increase our ability to separate closely spaced reflectors.

There is also a close relation between the length of a seismic source pulse as a function of time and it's frequency spectrum. We can easily see this in the case of a low-pass filter, where equation 3.32 gave the time-function

$$h(t) = 2f_0 \frac{\sin(2\pi f_0 t)}{2\pi f_0 t}. \tag{4.15}$$

$h(t)$ is a band-limited time function since the highest frequency corresponds to the cut-off frequency for the low-pass filter, f_0. If we define the length of $h(t)$ as the distance from $t = 0$ to the first zero-crossing we get that the length is defined by $2f_0T_L = 1$, since $\sin(\pi) = 0$. From this equation we see that the larger the cut-off frequency f_0 is, the shorter the length T_L becomes. In the limit of a very large f_0, the length of $h(t)$ approaches zero, i.e. $h(t)$ approaches a delta function. In fact, the Fourier transform of a delta-function is

$$\Delta(f) = \int_{-\infty}^{+\infty} dt\, \delta(t) \exp(2\pi f t) = 1. \tag{4.16}$$

So a δ function has a constant spectrum for all frequencies.

Figures 4.10,4.11, 4.12 and 4.13 demonstrates clearly the relation between bandwidth and length in the time domain.

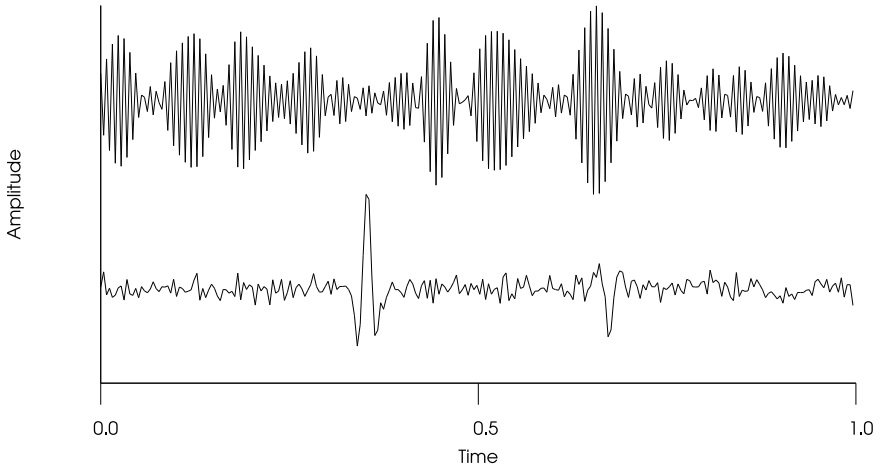

Figure 4.6: The input seismic data with added noise is shown in the lower trace, while the ouput of a spiking deconvolution filter applied to the input data is shown in the upper trace.

4.4 Shaping (Wiener) filters

Shaping filters, or Wiener filters, are a more general class of filters than the spiking deconvolution filter. A Wiener filter is designed to turn a given input seismic pulse $s(t)$ into a predetermined output pulse $g(t)$. In contrast to the spiking deconvolution filter described above it is designed completely in the time-domain, without using a Fourier transform.

Given the convolutional model for seismic data

$$a(t) = r(t) * s(t), \tag{4.17}$$

where $a(t)$ is the seismic data, $r(t)$ is the reflectivity and $s(t)$ is the seismic pulse, we want to find an inverse $s^{-1}(t)$ such that

$$s^{-1}(t) * s(t) = \delta(t). \tag{4.18}$$

A slightly more general approach would be

$$f(t) * s(t) = g(t), \tag{4.19}$$

where $f(t)$ is an inverse transforming $s(t)$ into a desired time function $g(t)$.

In general, if $f(t)$ is not perfect, there will be some difference between our desired output $g(t)$ and the actual output $\hat{g}(t)$. The error between the actual and the desired output can be measured by the *mean-square error* defined by

$$e = \frac{1}{T} \int_{-\infty}^{+\infty} [g(t) - \hat{g}(t)]^2, \tag{4.20}$$

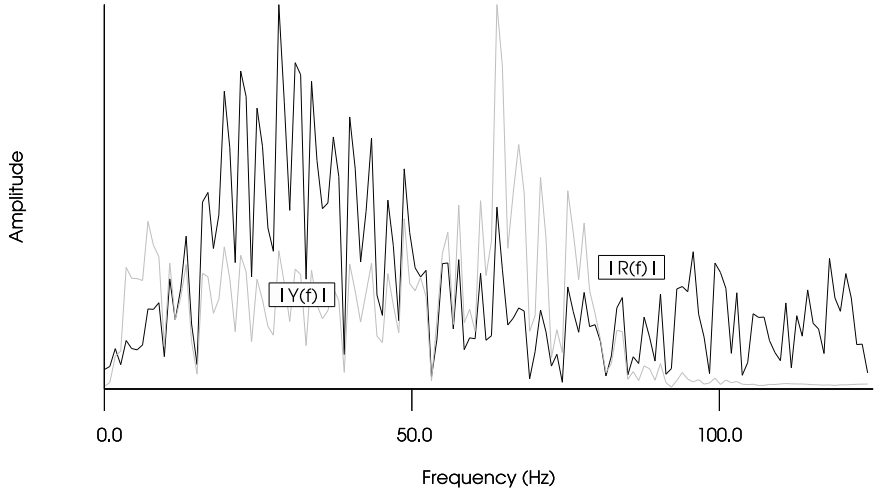

Figure 4.7: The spectrum of the input data with added noise $|Y(f)+N(f)|$ and the stabilized deconvolved output $|R(f)|$ (gray line).

or if the functions above are sampled

$$e = \frac{1}{N}\sum_{k=0}^{N}[g_k - \hat{g}_k]^2. \tag{4.21}$$

We will now try to find a filter f_k such the error e is as small as possible. This will be our definition of a Wiener filter, a filter which minimizes the difference between the desired output and the actual output.

The output from the (yet) unknown filter in terms of the input is given by a convolution

$$\hat{g}_k = \sum_{l=0}^{M} s_{k-l} f_l, \tag{4.22}$$

Where M is the length of the Wiener filter, or the number of filter coefficients. By using equation 4.21 the corresponding mean square error is

$$e = \frac{1}{N}\sum_{k=0}^{N}\left[g_k - \sum_{l=0}^{M} s_{k-l} f_l\right]^2. \tag{4.23}$$

Equation 4.23 expresses the error-energy as a function of the filter coefficients f_k since everything else is known. To find the filter coefficients which minimizes the energy we require that

$$\frac{\partial e}{\partial f_m} = 0, \tag{4.24}$$

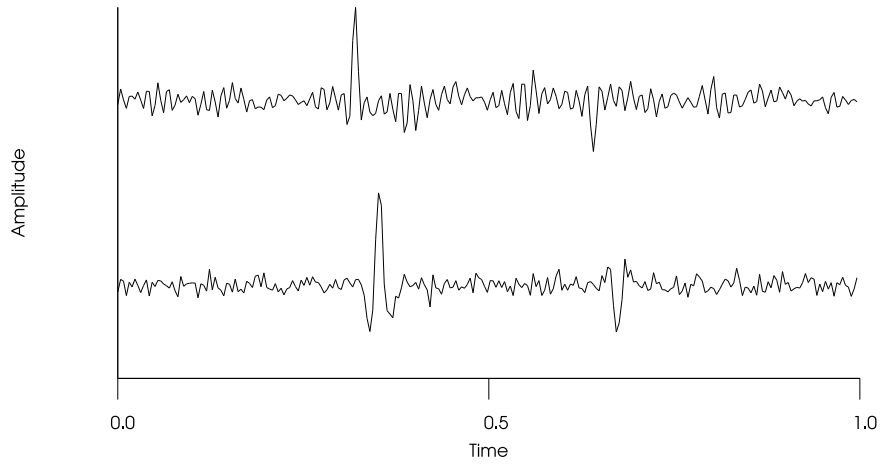

Figure 4.8: The input seismic data is shown in the lower trace, while the ouput of a stabilized spiking deconvolution filter applied to the input data is shown in the upper trace.

for $m = 0, 1, 2, ..., M$. Applying this to equation 4.23, we get

$$0 = \frac{-2}{N} \sum_{k=0}^{N} \left[g_k - \sum_{l=0}^{M} s_{k-l} f_l \right] s_{k-m}. \tag{4.25}$$

The last equation becomes after reorganizing and multiplication with $-2/N$ on both sides

$$0 = \sum_{k=0}^{N} g_k s_{k-m} - \sum_{k=0}^{N} \sum_{l=0}^{M} s_{k-l} s_{k-m} f_l, \tag{4.26}$$

or

$$\sum_{k=0}^{N} g_k s_{k-m} = \sum_{l=0}^{M} \sum_{k=0}^{N} s_{k-l} s_{k-m} f_l. \tag{4.27}$$

To simplify equation 4.27, we introduce the *cross correlation*

$$\phi_{gs}(m) = \sum_{k=0}^{N} g_k s_{k-m}, \tag{4.28}$$

and the *autocorrelation*

$$\phi_{ss}(m) = \sum_{k=0}^{N} s_k s_{k-m}, \tag{4.29}$$

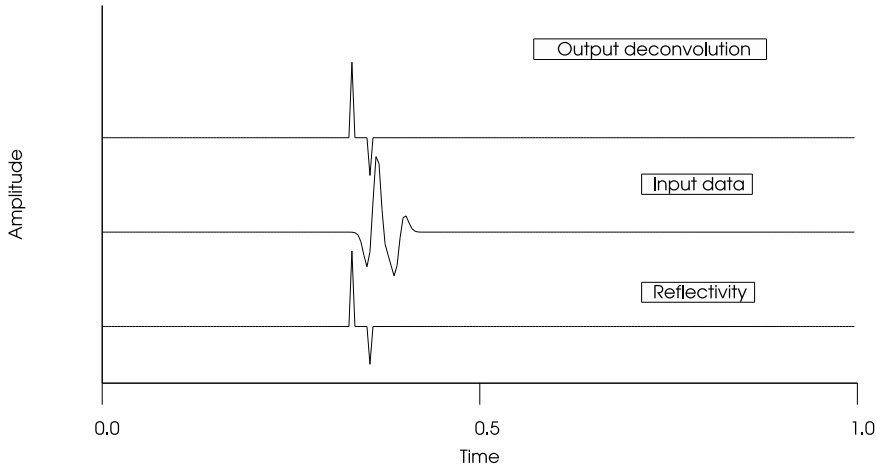

Figure 4.9: The lower trace shows the input reflectivity function used to create the synthetic data shown in the middle trace. The output of a spiking deconvolution filter applied to the input data is shown in the upper trace.

Equation 4.27 then becomes

$$\phi_{gs}(m) = \sum_{l=0}^{M} \sum_{k=0}^{N} s_{k-l} s_{k-m} f_l. \tag{4.30}$$

On the right hand side, we can make a change of the summation variable $k' = k - l$ which gives $k = k' + l$

$$\phi_{gs}(m) = \sum_{l=0}^{M} \sum_{k'=-l}^{N-l} s_{k'} s_{k'-(m-l)} f_l. \tag{4.31}$$

Assuming that $s'_k = 0$ for $k' < 0$ and that $s_k = 0$ for $k > N - l$ the last equation can be expressed as

$$\phi_{gs}(m) = \sum_{l=0}^{M} \phi_{ss}(m-l) f_l, \tag{4.32}$$

for $m = 0, 1, , , , M$. Equation 4.32 is known as Levinson's *normal equations*. The normal equations can be solved efficiently, resulting in a reasonably fast method for computing a Wiener filter.

Figure 4.14 shows the output of a Wiener filter with the desired output $\hat{g}(t) = \delta(t)$ and the input $s(t)$ equal to a Ricker pulse. Clearly, the Wiener filter does not perform very well. The problem is that the Wiener filter turns out to work better if the input seismic pulse is so-called *minimum-phase*. A

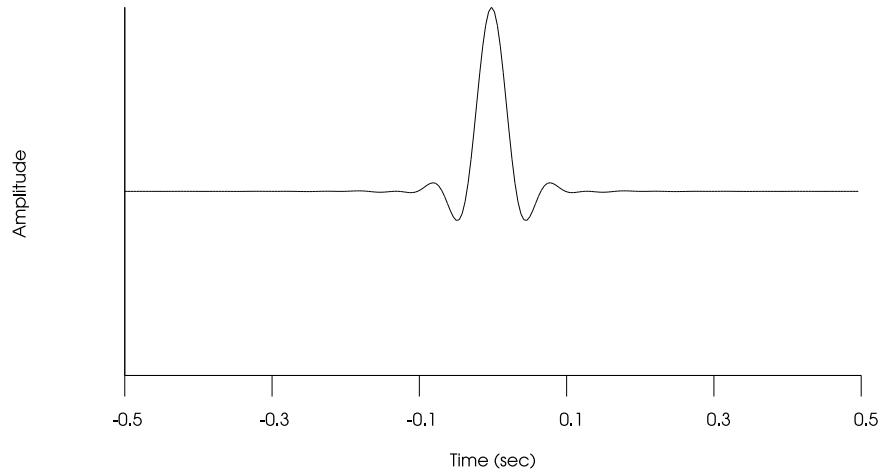

Figure 4.10: The impulse response of the low-pass filter shown in figure 4.11.

minimum-phase time function, $s(t)$, fulfills the following properties

$$s(t) = 0 \text{ for } t < 0, \tag{4.33}$$

$$\int_0^{+\infty} s^2(t) \text{ is finite}, \tag{4.34}$$

$$s^{-1}(t) = 0 \text{ for } t < 0 \tag{4.35}$$

$$\int_0^{+\infty} [s^{-1}(t)]^2 \text{ is finite}. \tag{4.36}$$

$$\tag{4.37}$$

A Ricker pulse violates the rules above. If we change the seismic pulse to a time function which is minimum-phase, the result corresponding to Figure 4.14 is shown in Figure 4.15. We see that the filter now performs much better. Figure 4.16 shows the result corresponding to Figure 4.15 but with noise added. We see that the result is reasonably good.

4.5 Minimum phase and Wiener inverse filters

The z-transform

A useful representation of time series is the z-transform. The z-transform of a sampled function a_k is defined by

$$A(z) = \sum_{k=0}^{N} a_k z^k, \tag{4.38}$$

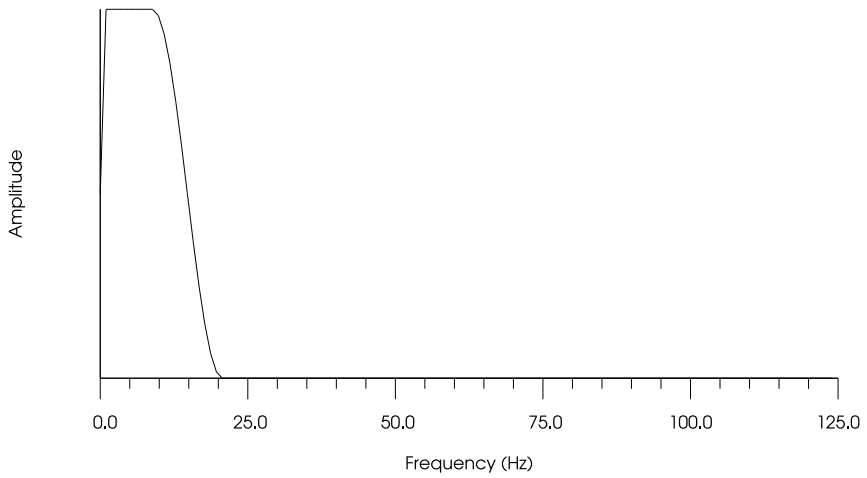

Figure 4.11: Low-pass filter with cutoff at 20 Hz.

where multiplication with z corresponds to a time delay of one sample, multiplication with z^2 corresponds to a time delay of two samples, and so one.

Multiplication of two z-transform corresponds to convolution in time domain, which is seen by considering the convolution of two time-series a_k and b_k

$$c_k = \sum_{l=0}^{N} a_l b_{k-l}. \tag{4.39}$$

We now have that

$$\begin{aligned} c_0 &= a_0 b_0, \\ c_1 &= a_0 b_1 + a_1 b_0, \\ c_2 &= a_0 b_2 + a_1 b_1 + a_2 b_0, \\ &\cdots \\ c_{2N} &= a_N b_N, \end{aligned} \tag{4.40}$$

On the other hand the product of the two z-transforms $A(z)$ and $B(z)$ is

$$A(z)B(z) = \left(\sum_{k=0}^{N} a_k z^k \right) \left(\sum_{k=0}^{N} a_b z^k \right), \tag{4.41}$$

which becomes

$$\begin{aligned} A(z)B(z) = &\left(a_0 + a_1 z + a_2 z^2 + \ldots a_N z^N\right) \times \\ &\left(b_0 + b_1 z + b_2 z^2 + \ldots + b_N z^N\right), \end{aligned} \tag{4.42}$$

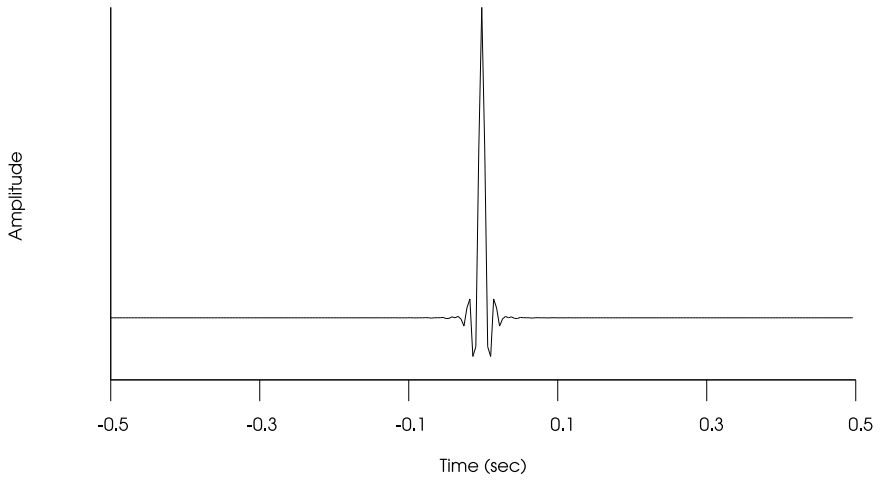

Figure 4.12: The impulse response of the low-pass filter shown in figure 4.13.

which is

$$\begin{aligned} A(z)B(z) &= a_0b_0 + (a_0b_1 + a_1b_0)z \\ &+ (a_2b_0 + a_1b_1 + a_0b_2)z^2 + \ldots + a_Nb_Nz^{2N}. \end{aligned} \tag{4.43}$$

From the definition of the z-transform and equation 4.40 we have the z-transform of c

$$\begin{aligned} C(z) &= a_0b_0 + (a_0b_1 + a_1b_0)z \\ &+ (a_2b_0 + a_1b_1 + a_0b_2)z^2 + \ldots + a_Nb_Nz^{2N}. \end{aligned} \tag{4.44}$$

Comparing equation 4.44 and equation 4.43 we see that

$$C(z) = A(z)B(z). \tag{4.45}$$

This result is the same as for the Fourier transforms of two time series. In fact if we set $z = \exp(2\pi i\Delta tf)$, then the z-transform is the same as the Discrete Fourier Transform, which is seen by putting $f = n/T$, where T is the period.

Minimum phase

To explain the concept of minimum phase consider a very simple pulse shape with only two samples $s_k = (s_0, s_1)$. The z-transform is then

$$S(z) = s_0 + s_1z. \tag{4.46}$$

The inverse of $S(z)$ is

$$S^{-1}(z) = \frac{1}{(s_0 + s_1z)} = \frac{1}{s_0\left[1 + (s_1/s_0)\,z\right]}. \tag{4.47}$$

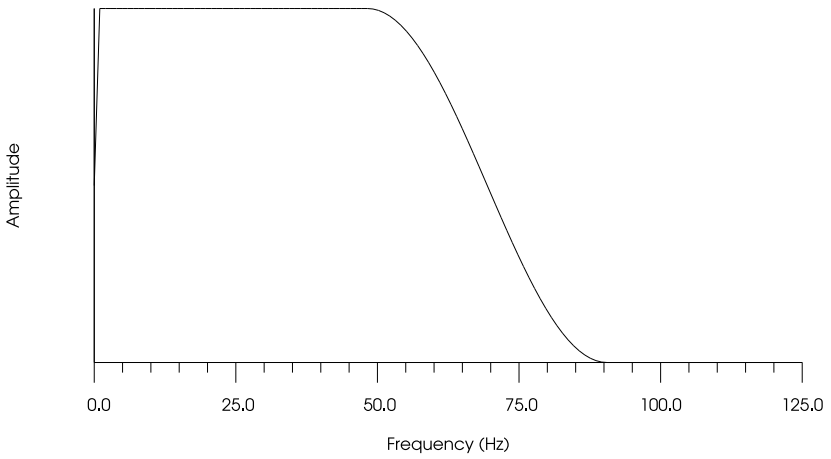

Figure 4.13: Low-pass filter with cutoff a 90 Hz.

According to Rottman (1960) the following formula holds

$$\frac{1}{1+x} = 1 - x + x^2 - x^3 + \dots \tag{4.48}$$

Using equation 4.48 in 4.47 gives

$$S^{-1}(z) = \frac{1}{s_0}\left[1 - \frac{s_1}{s_0}z + \left(\frac{s_1}{s_0}\right)^2 z^2 - \left(\frac{s_1}{s_0}\right)^3 z^3 + \dots\right] \tag{4.49}$$

The series on the right only converges if $s_0 > s_1$. If $s_0 < s_1$ it is possible to expand $S(z)$ in negative powers of z:

$$S^{-1}(z) = \frac{1}{z s_1 \left[1 + (s_0/s_1)\, z^{-1}\right]} \tag{4.50}$$

$$S^{-1}(z) = \frac{1}{z s_1}\left[1 - \frac{s_0}{s_1}z^{-1} + \left(\frac{s_0}{s_1}\right)^2 z^{-2} - \left(\frac{s_0}{s_1}\right)^3 z^{-3} + \dots\right] \tag{4.51}$$

The right hand side of equation 4.51 only converges if $s_0 < s_1$. However equation 4.51 involves only negative powers of z, which implies that $s^{-1}(t) \neq 0$ for $t < 0$. According to our definition of minimum-phase we required that $s^{-1}(t) = 0$ for $t < 0$. In this case this implies that for our trial seismic pulse $s_0 > s_1$ for the minimum-phase requirement to be fulfilled.

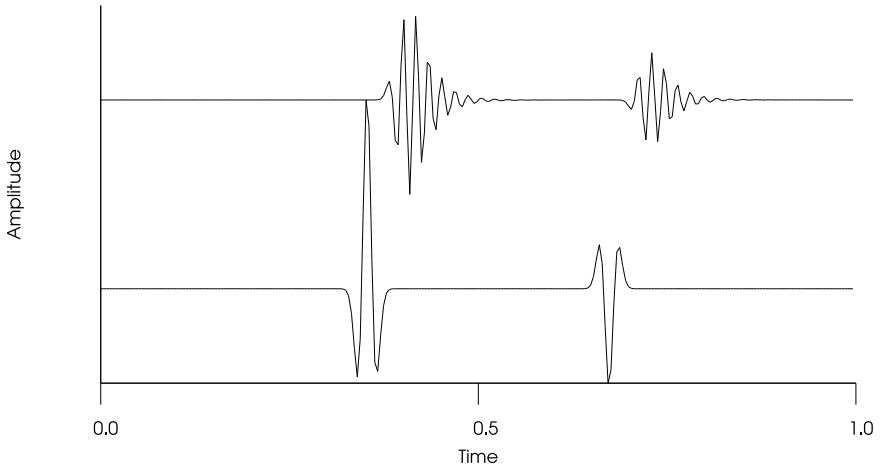

Figure 4.14: The input synthetic seismic data is shown in the lower trace, while the ouput of applying a Wiener filter is shown in the upper trace.The seismic pulse is a Ricker pulse, which is not minimum phase.

The Fourier transform of $s(t)$ is found by putting $z = \exp(2\pi i f \Delta t)$ in the z-transform:

$$S(f) = s_0 + s_1 \exp(2\pi i f \Delta t). \tag{4.52}$$

$S(f)$ can be written as a combination of amplitude and phase-spectrum

$$S(f) = |S(f)| \exp[i\phi(f)], \tag{4.53}$$

where the amplitude spectrum is

$$|S(f)|^2 = s_0^2 + 2s_0 s_1 \cos(2\pi \Delta t f) + s_1^2, \tag{4.54}$$

and the phase spectrum is

$$\tan[\phi(f)] = \frac{\mathrm{Im}S(f)}{\mathrm{Re}S(f)} = \frac{s_1 \sin(2\pi f \Delta t)}{s_0 + s_1 \cos(2\pi f \Delta t)}, \tag{4.55}$$

which is

$$\tan[\phi(f)] = \frac{\mathrm{Im}S(f)}{\mathrm{Re}S(f)} = \frac{\sin(2\pi f \Delta t)}{[(s_0/s_1) + \cos(2\pi f \Delta t)]}. \tag{4.56}$$

We see very clearly that if $s_0 > s_1$ then $\phi(f) = \phi_{min}(f)$ is less than $\phi(f) = \phi_{max}(f)$ corresponding to the case when $s_0 < s_1$. However, note that the amplitude spectrum is unchanged no matter values of s_0 and s_1. So there is a range of different waveforms with different phases corresponding to what

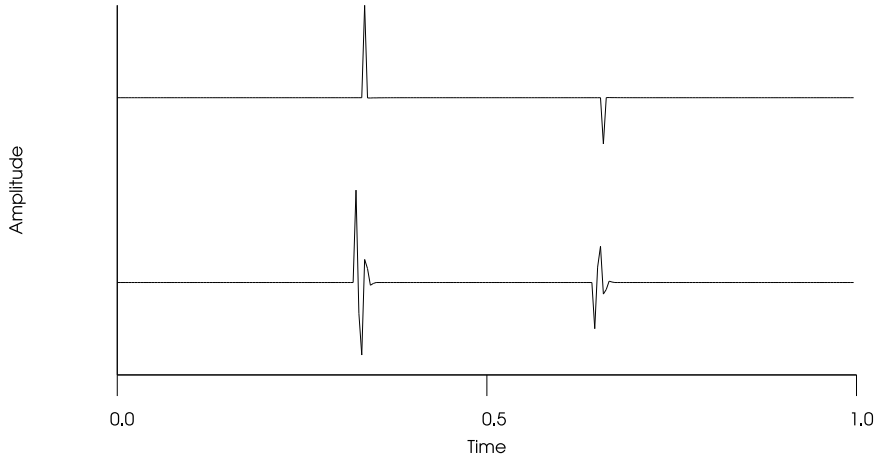

Figure 4.15: The input synthetic seismic data is shown in the lower trace, while the ouput of applying a Wiener filter is shown in the upper trace.The seismic pulse is minimum-phase.

choices are made for s_0 and s_1. A conventional classification would be to call $s(t)$ minimum phase if $s_0 > s_1$, maximum phase if $s_0 < s_1$ and mixed-phase if $s_0 = s_1$. Note that the phase is never zero for all frequencies. To obtain a pulse form with zero-phase one would have to add negative powers of z, i.e the pulse form is no longer causal. The choice $S(Z) = s_1 z^{-1} + s_0 + s_1 z$ would lead to $\phi(f) = 0$ for all f.

4.6 Statistical properties of Time series

A transient signal exists for a finite length of time. A time series

$$a_k = a_0, a_1, \ldots, a_N \tag{4.57}$$

with $N + 1$ samples is an example of a transient time series. The energy of a transient time series is defined by

$$E_a = \sum_{k=0}^{N} a_k^2. \tag{4.58}$$

. We can also define the *power* of a time series as

$$P_a = \frac{1}{N+1} \sum_{k=0}^{N} a_k^2. \tag{4.59}$$

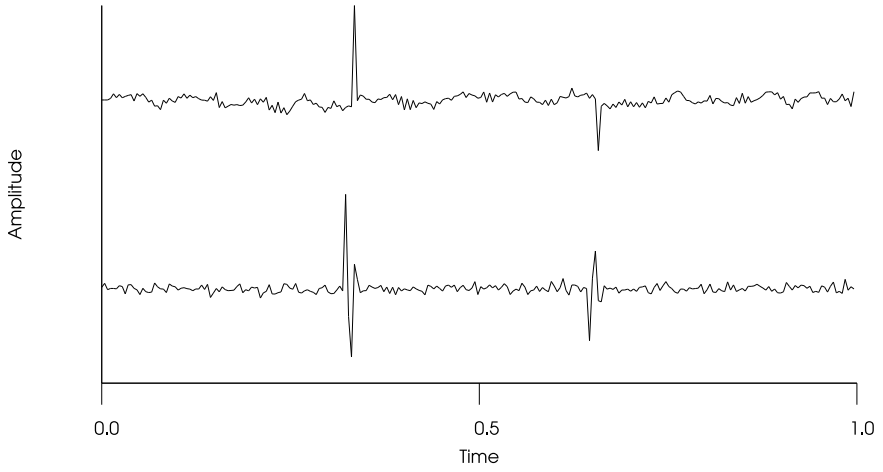

Figure 4.16: The input synthetic seismic data with added noise is shown in the lower trace, while the ouput of applying a Wiener filter is shown in the upper trace.The seismic pulse is minimum-phase.

The *mean* value of a time series is

$$\bar{a}_k = \frac{1}{N}\sum_{k=0}^{N} a_k. \tag{4.60}$$

The standard deviation σ and the variance σ^2 is defined by

$$\sigma^2 = \frac{1}{N+1}\sum_{k=}^{N}(a_k - \bar{a}_k)^2. \tag{4.61}$$

Equations 4.59, 4.60 and 4.61 also holds for infinitely long time series in the limit when N approaches ∞.

We defined the cross-correlation between two time series a_k and b_k as

$$\phi_{ab}(m) = \sum_{k=0}^{N} a_k b_{k-m}, \tag{4.62}$$

and the auto-correlation

$$\phi_{aa}(m) = \sum_{k=0}^{N} a_k a_{k-m}. \tag{4.63}$$

For infinitely long time series the cross and autocorrelation would have to be modified to

$$\phi_{ab}(m) = \frac{1}{N+1}\sum_{k=0}^{N} a_k b_{k-m}, \tag{4.64}$$

and the auto-correlation

$$\phi_{aa}(m) = \frac{1}{N+1}\sum_{k=0}^{N} a_k a_{k-m}, \tag{4.65}$$

and it would then be understood that equations 4.64 and 4.65 exists in the limit when N approaches infinity.

The corresponding cross-correlation for continuous functions is

$$\phi_{ab}(t) = \int_{-\infty}^{+\infty} d\tau\, a(\tau)b(\tau - t), \tag{4.66}$$

which is the same as

$$\phi_{ab}(t) = \int_{-\infty}^{+\infty} d\tau\, a(\tau + t)b(\tau). \tag{4.67}$$

The last equation is proved by substitution of variables by $u = \tau - t$.

The auto-correlation becomes

$$\phi_{aa}(t) = \int_{-\infty}^{+\infty} d\tau\, a(\tau)a(\tau + t). \tag{4.68}$$

The Fourier transform of equation 4.67 is

$$\Phi_{ab}(f) = \int_{-\infty}^{+\infty} dt \int_{-\infty}^{+\infty} d\tau\, \exp(-2\pi i f t)a(\tau + t)b(\tau), \tag{4.69}$$

which becomes after a change of variable $u = \tau + t$:

$$\Phi_{aa}(f) \int_{-\infty}^{+\infty} d\tau\, [\exp(2\pi i f \tau)b(\tau)]^* \int_{-\infty}^{+\infty} du\, \exp(-2\pi i f u)a(u), \tag{4.70}$$

which is the same as

$$\Phi_{ab}(f) = A(f)B^*(f). \tag{4.71}$$

If $a = b$ we get

$$\Phi_{aa}(f) = A(f)A^*(f) = |A(f)A^*(f)|^2. \tag{4.72}$$

The Fourier transform of the auto-correlation is the square of the amplitude spectrum, which is also called the power spectrum.

If a time-series is *white*, the amplitude spectrum is equal to a constant. A *stationary* time series is infinitely long and all the statistical properties defined above are independent on time, including mean value and auto-correlation. A *white* and em stationary time series has both these properties.

If the autocorrelation is given by the time function

$$\phi_{aa}(t) = \sigma^2\delta(t), \tag{4.73}$$

the Fourier transform of equation 4.73 is

$$\Phi_{aa}(f) = \int_{-\infty}^{+\infty} \exp(-2\pi f t)\sigma^2\delta(t) = \sigma^2. \tag{4.74}$$

The autocorrelation in equation 4.73 has a constant amplitude spectrum, and can be identified with the autocorrelation with a white, random and stationary time series. If the time series has zero mean value σ^2 can be identified as the variance,

4.7 Statistical spiking deconvolution

In order to use the Wiener inverse filter for spiking deconvolution the seismic source pulse need to be known. In many cases is a good estimate of the seismic source pulse difficult to obtain. However, by assuming that the reflectivity is stationary, white and random it is possible to get around this restriction and perform spiking deconvolution without knowing the seismic source pulse. The key observation is that the autocorrelation of the seismic data can be related to the autocorrelation of the seismic pulse.

First, the convolutional model gives the relation between the seismic data, $y(t)$, the reflectivity, $r(t)$, and the seismic source pulse

$$y(t) = r(t) * s(t). \tag{4.75}$$

In the frequency domain this is

$$Y(f) = R(f)S(f), \tag{4.76}$$

which by multiplying both sides with $Y^*(f)$ gives

$$\Phi_{yy}(f) = Y(f)Y^*(f) = R(f)S(f)[R(f)S(f)]^*, \tag{4.77}$$

or by rearranging

$$\Phi_{yy}(f) = Y(f)Y^*(f) = R(f)R^*(f)S(f)S^*(f). \tag{4.78}$$

This is equal to

$$\Phi_{yy}(f) = Y(f)Y^*(f) = \Phi_{rr}(f)\Phi ss(f), \tag{4.79}$$

where

$$\begin{aligned} \Phi_{rr} &= R(f)R^*(f), \\ \Phi_{ss} &= S(f)S^*(f). \end{aligned} \tag{4.80}$$

Fourier transformation back to time gives

$$\phi_{yy}(t) = \phi_{rr}(t) * \phi_{ss}(t), \tag{4.81}$$

where $\phi_{rr}(t)$ and $\phi_{ss}(t)$ are the autocorrelations of the reflectivity and the seismic source pulse, respectively. The crucial step now is to assume that the reflectivity, $r(t)$, is a stationary, white, random and with zero mean value. From equation 4.73 this implies

$$\phi_{rr}(t) = \sigma^2 \delta(t). \tag{4.82}$$

Inserting equation 4.82 into 4.81 gives

$$\phi_{yy}(t) = \sigma^2 \delta(t) * \phi_{ss}(t) = \sigma^2 \phi_{ss}(t). \tag{4.83}$$

The autocorrelation of the data is equal to the autocorrelation of the seismic source pulse, except for a constant factor! This is a major simplification.

The Wiener inverse filter given by equation 4.32 now becomes

$$\phi_{gs}(m) = 1/\sigma^2 \sum_{l=0}^{M} \phi_{yy}(m-l) f_l. \tag{4.84}$$

There is still the problem of the cross-correlation between the desired output $g(t)$ and the seismic source. The cross-correlation is

$$\phi_{gs}(m) = \sum_{l=0}^{N} g_l s_{l-m}. \tag{4.85}$$

Since the desired output is a delta function at time=1, the above cross-correlation is

$$\begin{aligned} \phi_{gs}(0) &= s_0, \\ \phi_{gs}(1) &= 0, \\ \phi_{gs}(1) &= 0, \\ &\cdots \\ &\cdots \\ &\cdots \\ \phi_{gs}(N) &= 0. \end{aligned} \tag{4.86}$$

Inserting the last result back unto equation 4.84 gives the following system of equations after multiplying all equations with $1/s_0$

$$\begin{aligned} 1 &= 1/(s_0\sigma^2) \sum_{l=0}^{M} \phi_{yy}(-l) f_l, \\ 0 &= 1/(s_0\sigma^2) \sum_{l=0}^{M} \phi_{yy}(1-l) f_l, \\ &\cdots \\ 0 &= 1/(s_0\sigma^2) \sum_{l=0}^{M} \phi_{yy}(N-l) f_l. \end{aligned} \tag{4.87}$$

Except for the scale factor $1/(s_0\sigma^2)$, all quantities in equation 4.87 are known. The scale factor will only influence the absolute value of the filter, and not the shape.

Figure 4.17 shows a simple reflectivity model and the corresponding seismic data, while figure 4.18 shows the autocorrelation of the reflectivity and the seismic data. Note that the autocorrelation of the reflectivity is a single impulse at time equal zero, while the autocorrelation of the input data extends from -20 ms to + 20 ms. From figure 4.18 we see that the autocorrelation of the

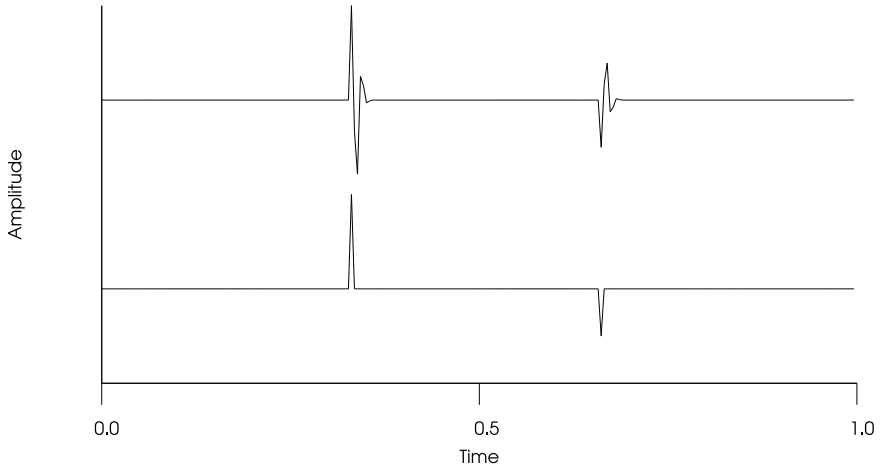

Figure 4.17: Reflectivity model (lower trace) and the corresponding seismic data (upper trace).

input data is zero for all time-lags larger than $\pm$20 ms. We need only to solve equation 4.87 for values of $M\Delta t < 40ms$, since for any large value of M, the filter coefficients are zero. Figure 4.19 shows the result of performing spiking deconvolution of the data shown in figure 4.17 and using the autocorrelation shown in figure 4.18.

4.8 Inverse filter for multiples

Multiple reflections (multiples) is usually considered as unwanted signal in seismic processing. Multiples generated by the water layer in marine seismics is particularly troublesome because of the large reflection coefficient of the sea surface. Figure 4.20 shows a simplified drawing of ray paths for multiples reflected from the surface and the sea bottom. If we consider only vertically traveling waves, the two-way traveltime in the water layer is τ, the reflection coefficient at the bottom of the layer is r and the reflection coefficient at the top

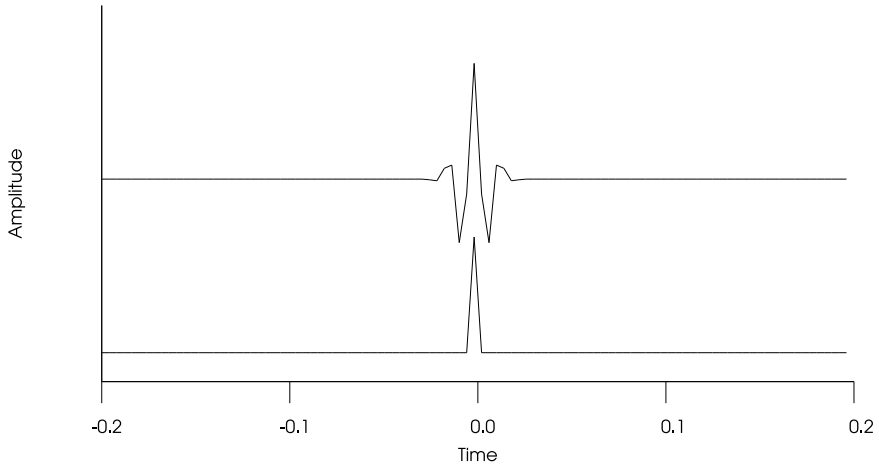

Figure 4.18: Autocorrelation of reflectivity model(lower trace) shown in figure 4.17 and the corresponding autocorrelation for the seismic data (upper trace) shown in figure 4.17.

of the layer is -1, we can formulate a simple model for the multiples

$$y(t) = rs(t-\tau) - r^2 s(t-2\tau) + r^3 s(t-3\tau) + \ldots \tag{4.88}$$

Taking the Fourier transform of equation 4.88, one gets

$$Y(f) = rS(f)\exp(-2\pi f\tau) - r^2 S(f)\exp(-4\pi f\tau) + r^3\exp(-6\pi f\tau) + \ldots \tag{4.89}$$

If we set $R = r\exp(-2\pi f\tau]$, then equation 4.89 is:

$$Y(f) = S(f)R\left[1 - R + R^2 + \ldots\right]. \tag{4.90}$$

The right hand side of equation 4.90 is recognized as an infinite geometrical series,

$$\frac{1}{1+x} = 1 - x + x^2 - x^3 + \ldots \tag{4.91}$$

implying that equation 4.90 can be written

$$Y(f) = \frac{S(f)R}{1+R}. \tag{4.92}$$

Multiplying both sides with $1/(1-R)$ we get

$$(1+R)Y(f) = S(f)R. \tag{4.93}$$

We recognize the right hand side as the primary reflection, so we understand that the filter $1-R$ operating on the data on the left hand side actually removes all multiple reflections originally present in the data.

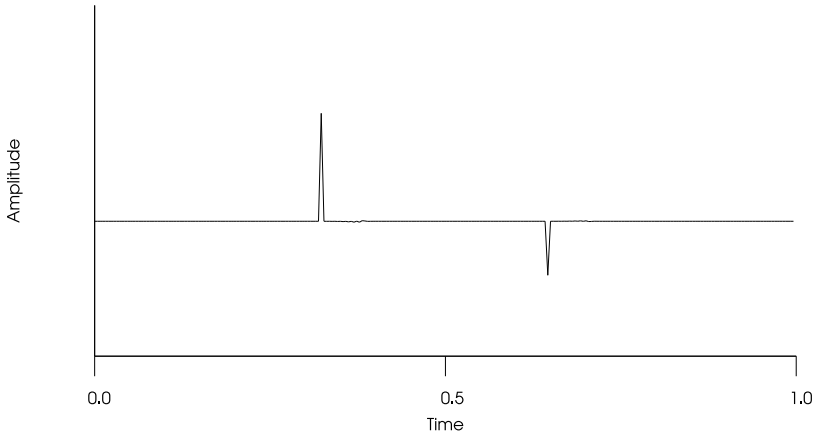

Figure 4.19: Statistical spiking deconvolution of the input data shown in 4.17.

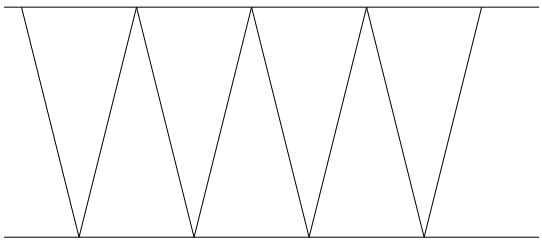

Figure 4.20: Raypaths for multiple reflections

Now consider the Fourier transform of equation 4.93. The right hand side has a Fourier transform (inserting $R = r\exp(-2\pi f\tau]$)

$$\int_{-\infty}^{+\infty} df\, S(f)\exp(2\pi ift) r\exp(-2\pi f\tau) = rs(t-\tau). \tag{4.94}$$

The left hand side is a product of $Y(f)$ and $1+R$, so the Fourier transform is going to be a convolution of the Fourier transforms of these two factors. The Fourier transform of $Y(f)$ is $y(t)$, while the Fourier transform of $1+R$ is

$$\int_{-\infty}^{+\infty} df\ \exp(2\pi ift)\left[1 + r\exp(-2\pi f\tau)\right] = \int_{-\infty}^{+\infty} df\ \left\{\exp(2\pi ift) + r\exp[2\pi if(t-\tau)]\right\} \tag{4.95}$$

Making the change of variable $\omega = 2\pi f$, the last integral in equation 4.95 becomes

$$\frac{1}{2\pi}\int_{-\infty}^{+\infty} d\omega\ \left\{\exp(i\omega t) + r\exp[i\omega(t-\tau)]\right\}. \tag{4.96}$$

According to Rottman (1960), the delta function can be represented as

$$\delta(x-t) = \frac{1}{2\pi}\int_{-\infty}^{+\infty} dz\ \exp[iz(x-t)], \tag{4.97}$$

Implying that

$$\frac{1}{2\pi}\int_{-\infty}^{+\infty} d\omega\ \{\exp(i\omega t) + r\exp[i\omega(t-\tau)]\} = \delta(t) + r\delta(t-\tau). \tag{4.98}$$

Putting everything together, we get the Fourier transform of equation 4.95 as

$$rs(t-\tau) = y(t) * [\delta(t) + r\delta(t-\tau)]. \tag{4.99}$$

The left hand side is recognized as the primary reflection, and we can write

$$rs(t-\tau) = y_p(t) = y(t) * [\delta(t) + r\delta(t-\tau)]. \tag{4.100}$$

The simple filter of two δ functions then act as a multiple removal filter. To see how the filter works, we perform the convolution on the right hand side

$$y_p(t) = y(t) + ry(t-\tau). \tag{4.101}$$

The first multiple arrives at $t = 2\tau$, so that equation 4.101 gives

$$y_p(2\tau) = y(2\tau) + ry(\tau), \tag{4.102}$$

and we see that the operation on the right hand side consists of adding a scaled version of the primary reflection, $ry(\tau)$ from the multiple arrival. Since the polarity of the multiple is opposite to that of the primary, this will effectively zero out the multiple reflection. Figure 4.21 shows the application of the filter on synthetic data. The synthetic data consists of a primary reflection followed by three multiples. Note that the filter removes perfectly the three multiples, but it also generates an extra artificial reflection. The input data is not perfect, since it it truncated at the third multiple, and the filter then produces an artificial reflection. Because of this, and the fact that the reflection coefficient must be known, application of this method to real seismic data is difficult. However, the principle of using the fact that the noise is periodic to try to remove it, is interesting. We will pursue that in the next sections.

4.9 Predictive deconvolution

Prediction error filtering

A prediction filter predicts the input y_k at some future time $y_{k+\alpha}$. The predicted value is denoted by $\hat{y}_{k+\alpha}$ and is an estimate of the true value $y_{k+\alpha}$. The filter is assumed linear and we have

$$g_t = \hat{y}_{k+\alpha} = \sum_{l=0}^{N} p_l y_{k-l}. \tag{4.103}$$

We can find a Wiener prediction filter by solving the normal equations given by equation 4.32 by assuming that the given input is equal to y_k, while the desired output is a future value $y_{k+\alpha}$. The right hand side cross-correlation then becomes:

$$\phi_{gs}(m) = \sum_{l=m}^{N} y_{l+\alpha} y_{l-m}. \tag{4.104}$$

Making the change of variable $l' = l + \alpha$, the equation above is

$$\phi_{gs}(m) = \sum_{l'=\alpha+m}^{N} y_{l'} y_{l'-(m+\alpha)} = \phi_{yy}(m+\alpha). \tag{4.105}$$

The normal equations then become

$$\sum_{l=0}^{N} \phi_{yy}(l-m) f_l = \phi_{yy}(m+\alpha), \tag{4.106}$$

for $m = 0, 1, \ldots, N$.

The prediction error is defined by

$$\epsilon_k = y_{k+\alpha} - \hat{y}_{k+\alpha}. \tag{4.107}$$

The prediction error represents the non-predictable part of the input data y_k. If the input data is stationary, white and random with zero mean value, then we would have

$$\begin{aligned} \phi_{xx}(m) &= 0, \text{ for } m \neq 0, \\ \phi_{xx}(m) &= \sigma^2 \text{ for } m = 0. \end{aligned} \tag{4.108}$$

The right hand side of equation 4.106 is zero for nonzero values of the prediction distance and all filter coefficients would be zero, and the predicted value would be equal to zero, which is the mean value of the input data.

In equation 4.107 we can replace the predicted value with equation 4.103 and get

$$\epsilon_{k+\alpha} = y_{k+\alpha} - \sum_{l=0}^{N} p_l y_{k-l}. \tag{4.109}$$

For easier interpretation, we can take the z-transform of equation 4.107

$$\sum_{k=0}^{N} z^k \epsilon_{k+\alpha} = \sum_{k=0}^{N} z^k y_{k+\alpha} - \sum_{j=0}^{N} z^k \sum_{l=0}^{N} p_l y_{k-l}, \tag{4.110}$$

which is slightly rewritten as

$$z^{-\alpha} \sum_{k=0}^{N} z^{k+\alpha} \epsilon_{k+\alpha} = z^{-\alpha} \sum_{k=0}^{N} z^{k+\alpha} y_{k+\alpha} - \sum_{j=0}^{N} z^k \sum_{l=0}^{N} p_l y_{k-l}. \tag{4.111}$$

We now recognize the z-transforms of each function, and get

$$z^{-\alpha}E(z) = z^{-\alpha}Y(z) - P(z)Y(z). \tag{4.112}$$

The z-transform of the prediction error is then

$$E(z) = [1 - z^{\alpha}P(z)]Y(z). \tag{4.113}$$

The filter

$$E(z) = [1 - z^{\alpha}P(z)], \tag{4.114}$$

is the z-transform of the time-domain filter

$$e_k = 1, 0, 0, 0, 0, \ldots, 0, -p_0, -p_1, \ldots, -p_N, \tag{4.115}$$

where the filter contains $\alpha - 1$ zeros. In the continuous formulation one would get

$$e(t) = \delta(t) - p(t - \tau_{\alpha}), \tag{4.116}$$

where τ_{α} is the time-delay corresponding to the prediction distance α.

If $\alpha = 1$ it can be shown that the filter

$$p_k = 1, -p_0, -p_1, \ldots, -p_N, \tag{4.117}$$

is identical with the statistical Wiener spiking deconvolution filter.

Figure 4.22 shows the autocorrelation of the input data shown in figure 4.21, while Figure 4.23 shows the result of applying a prediction error filter to the input data shown in figure 4.21. Here we have chosen the prediction length α to be equal to the multiple period of 100 ms. The prediction-error filter predicts and subtracts the multiples from the primary reflection. The filter length, M, should be equal to the width of the main lobe of the autocorrelation, and in this case that is 40 ms.

Figure 4.24 shows a so-called Common midpoint gather from a seismic survey, where reflectors appear as horizontal (flat) events. The autocorrelation of the CDP is also shown in the same figure. Note that the autocorrelation shows significant peaks at multiples of approximately 120 ms, indicating that periodic multiples are present. Figure 4.25 shows the result of applying predictive deconvolution to the input CDP shown in figure 4.24. The prediction length α was set to 120 ms, while the length of the filter was set to 60 ms. Figure 4.26 shows a brute stack where predictive deconvolution has been applied to all CDP's input to the stack. The prediction length α and the filter length was in this case set to 120 ms.

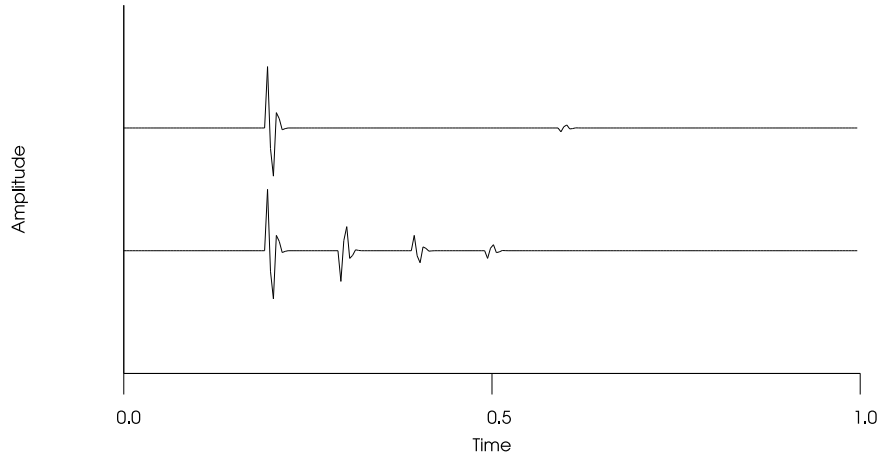

Figure 4.21: Input seismic data with multiples (lower trace) and output from multiple inverse filter (top)

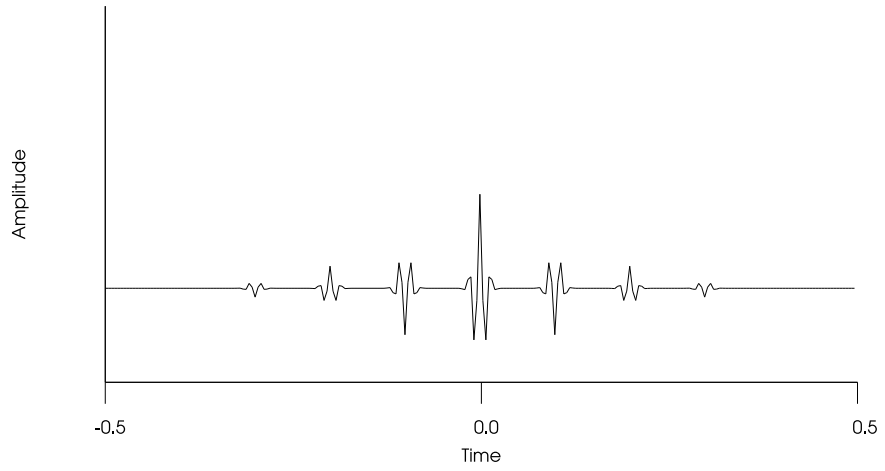

Figure 4.22: Autocorrelation of the input data shown in figure 4.21

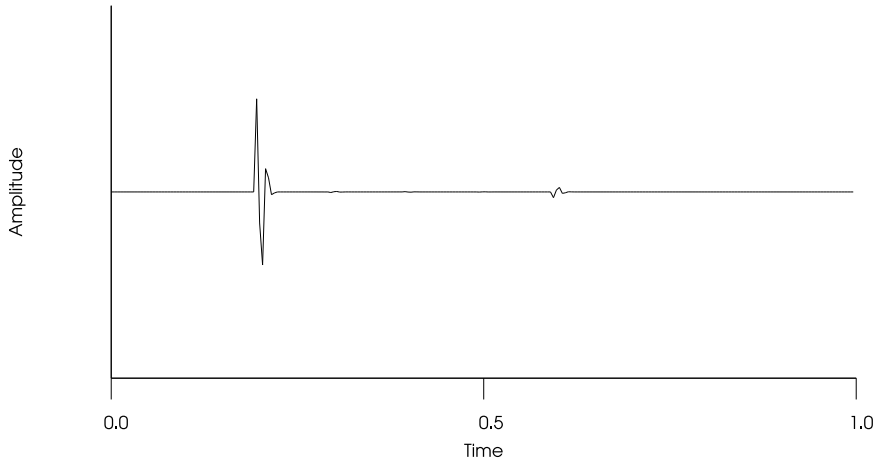

Figure 4.23: Prediction error filter applied to the input data shown in figure 4.21

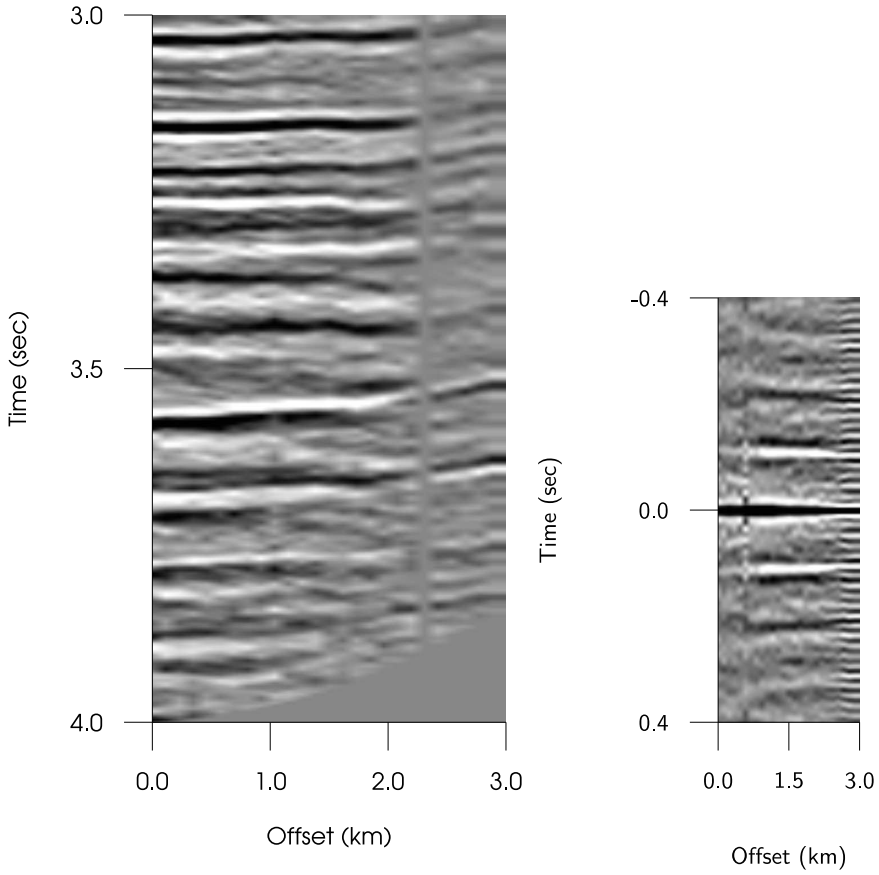

Figure 4.24: Input CDP-gather(left) and corresponding autocorrelation (right).

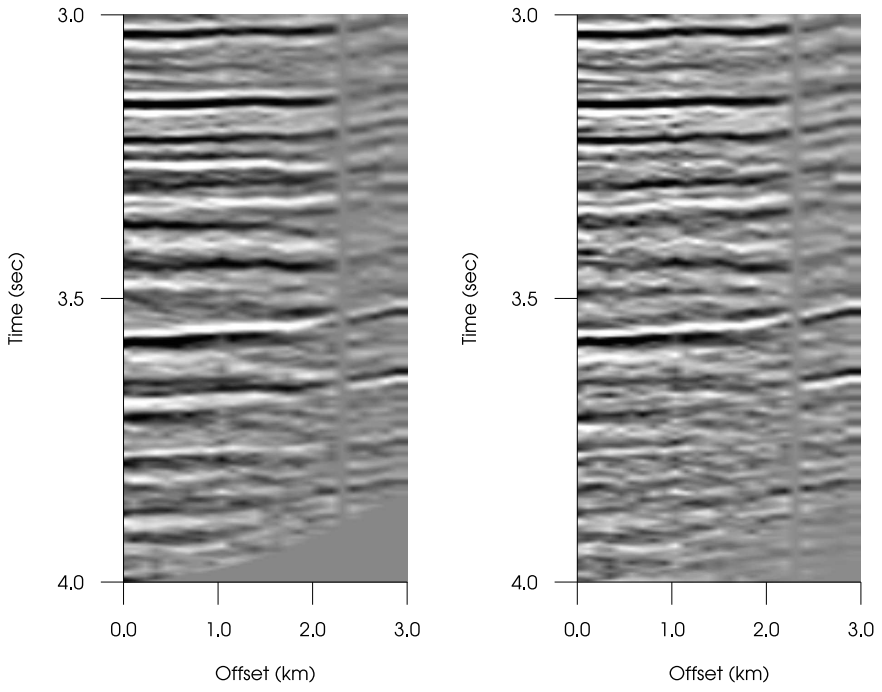

Figure 4.25: Input CDP gather (left) and CDP-gather after predictive deconvolution (right).

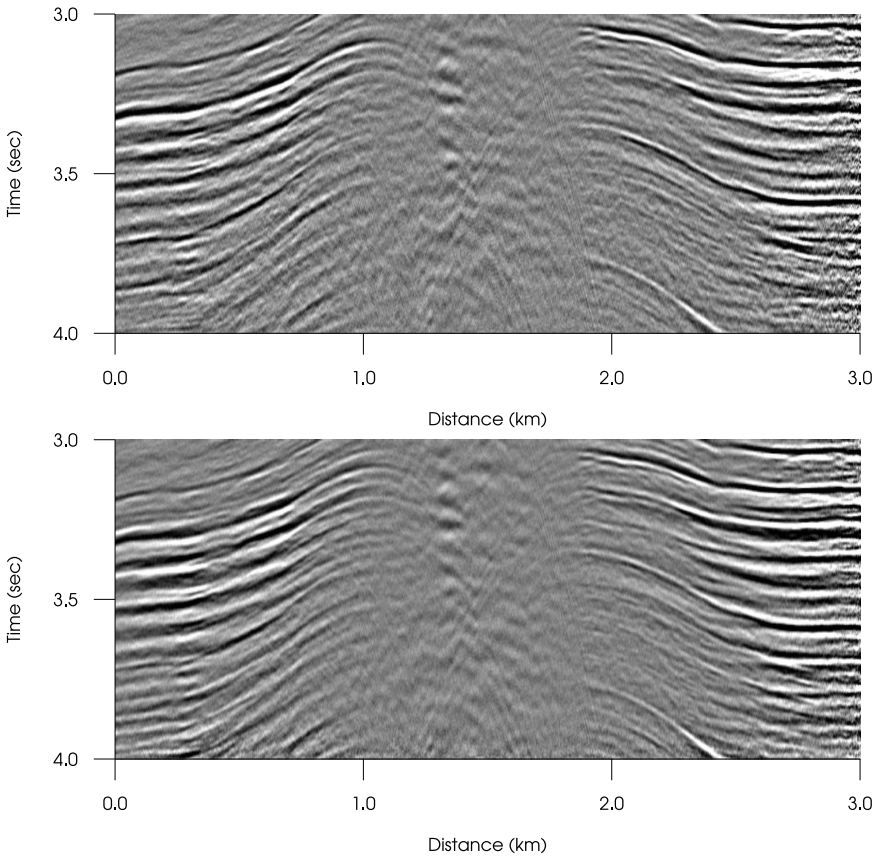

Figure 4.26: Brute stack (bottom) and brute stack after predictive deconvolution (top).

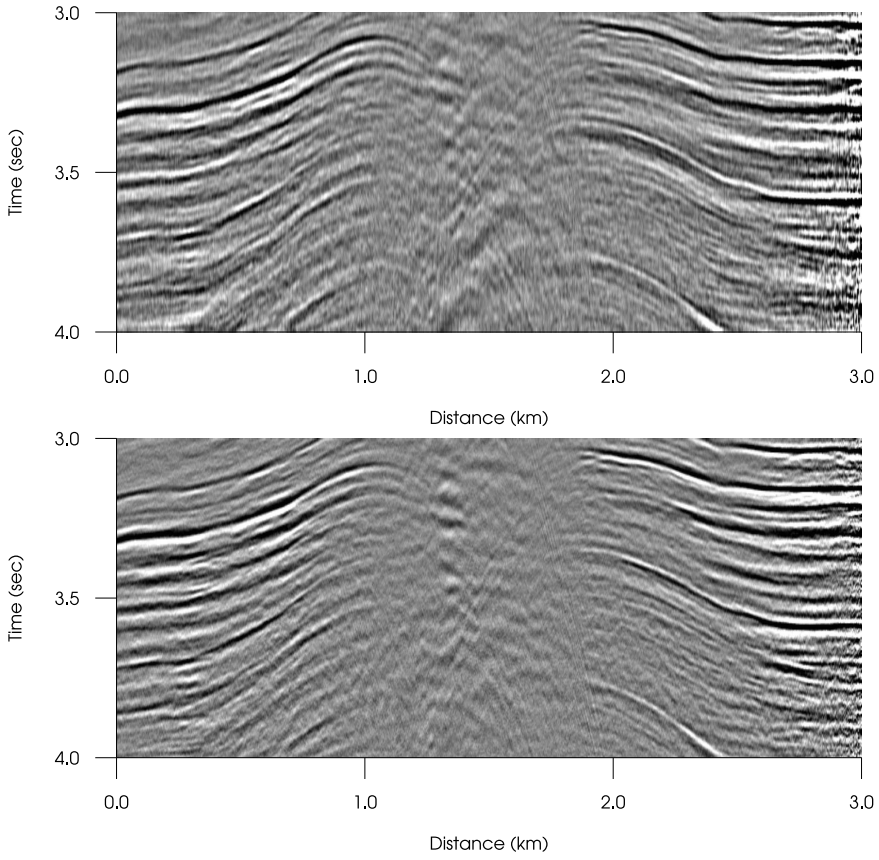

Figure 4.27: Brute stack after predictive deconvolution (bottom) and brute stack with predictive spiking deconvolution (top).